

The Response of Reinforced Concrete Composite Beams Reinforced with Pultruded GFRP to Repeated Loads

Teghreed H. Ibrahim *

Lecturer

Department of Civil Engineering,
University of Baghdad
Baghdad, Iraq

tagreed.hassan@coeng.uobaghdad.edu.iq

Abbas A. Allawi

Professor

Department of Civil Engineering,
University of Baghdad
Baghdad, Iraq

A.Allawi@uobaghdad.edu.iq

ABSTRACT

This paper investigates the experimental response of composite reinforced concrete with GFRP and steel I-sections under limited cycles of repeated load. The practical work included testing four beams. A reference beam, two composite beams with pultruded GFRP I-sections, and a composite beam with a steel I-beam were subjected to repeated loading. The repeated loading test started by loading gradually up to a maximum of 75% of the ultimate static failure load for five loading and unloading cycles. After that, the specimens were reloaded gradually until failure. All test specimens were tested under a three-point load. Experimental results showed that the ductility index increased for the composite beams relative to the reference specimen by 156.2% for a composite beam with GFRP with shear connectors, 148.6% for composite beams with GFRP without connectors, and 96% for the composite beam with a steel I-section.

Keywords: Pultruded GFRP I-beam, Repeated; Experiments, Deflections, Composite beam.

التصرف الإنشائي للعتبات الخرسانية المركبة مع المقطع البوليميري المقوى بألياف الزجاج تحت تأثير الحمل المتكرر

عباس عبد المجيد علاوي

أستاذ

قسم الهندسة المدنية/كلية الهندسة
جامعة بغداد

تغريد حسن ابراهيم*

مدرس

قسم الهندسة المدنية/كلية الهندسة
جامعة بغداد

الخلاصة

يبحث هذا البحث في الاستجابة التجريبية للخرسانة المسلحة المركبة باستخدام المقطع البوليميري GFRP والمقاطع الفولاذية تحت دورات محدودة من الحمل المتكرر. تضمن العمل التجريبي اختبار أربعة نماذج تكونت من نموذج مرجعي، واثنان من العتبات المركبة مع المقطع البوليميري GFRP I-section، وعتب خرساني مركب مع مقطع فولاذي على شكل I معرضه

*Corresponding author

Peer review under the responsibility of University of Baghdad.

<https://doi.org/10.31026/j.eng.2023.01.10>

This is an open access article under the CC BY 4 licenses (<http://creativecommons.org/licenses/by/4.0/>).

Article received: 15/8/2022

Article accepted: 31/10/2022

Article published: 1/1/2023



لأحمال تكرارية. بدأ اختبار التحميل المتكرر بالتحميل التدريجي بحد أقصى 75٪ من حمل الفشل الساكن النهائي لخمس دورات تحميل وتفريغ. بعد ذلك، تم إعادة تحميل العينات تدريجياً حتى الفشل. تم اختبار جميع عينات الاختبار تحت حمولة من ثلاث نقاط. أظهرت النتائج التجريبية أن مؤشر الليونة زاد للحمز المركبة بالنسبة للعينة المرجعية بنسبة 156.2٪ للحمزة المركبة مع GFRP بموصلات القص، و 148.6٪ للحمز المركبة مع GFRP بدون موصلات، و 96٪ للشعاع المركب مع الفولاذ. الكلمات الرئيسية: مقاطع بوليميرية، حمل متكرر، فحوص تجريبية، عتبات مركبة

INTRODUCTION

For recent research, the Glass Fiber Reinforced Polymer (GFRP) profiles were frequently utilized in composite beams because of their higher tensile performance, and many loading types have been done on this material. **(Ibrahim et al. 2022)** tested eight composite beams with pultruded GFRP under static and impact loading. Also, **(Ali and Allawi, 2021)** and **(Allawi and Ali 2020)** tested hybrid beams with GFRP under static and impact loading.

In recent decades, special attention has been paid to structures under repeated loads, such as railways and highway bridges. Limited research is related to composite concrete structures' behavior under repeated loads. A particular case of cyclic loading is repeated or half-cyclic loading, in which the loading is applied in unidirectional cycles.

(Sivagamasundari and Kumaran, 2008) evaluated the behavior of one-way slabs reinforced with GFRP bars and traditional reinforcement under cyclic loading with variable and constant amplitude fatigue loads. Eleven specimens have steel reinforcement, and 28 have GFRP. Seventeen of the 39 specimens were examined under variable-amplitude fatigue loading. Sixteen were tested under static load. The specimen is 2400mm long, 600mm wide, and 100mm to 120mm thick. Two concrete grades (20 MPa and 30 MPa) and three reinforcement percentages (0.65%, 0.82%, and 1.15%) were used. All slabs failed as flexural. At failure load, GFRP-reinforced slabs crushed concrete and fractured GFRP. (10–17%) of the slabs' flexural strength increased. by increasing compressive strength by 50% for the same slabs and slab thickness by 20% for the static load specimen. Increasing the compressive strength of concrete by 50% increased fatigue performance by 33% for the same slabs; GFRP reinforcement caused less damage than steel reinforcement. Also, slabs subjected to constant amplitude fatigue loading had a larger residual and final deflection and fracture width than slabs subjected to variable amplitude fatigue loading.

(Allawi and Jabir, 2016) tested nine RC one-way slabs with and without lacing reinforcement. The tests were designed to study the effect of the lacing reinforcement on the flexural response of one-way slabs under repeated load. The loading was applied as (5 cycles) loading-unloading to 80% of the ultimate load of the control specimen, then loaded up to the failure. Also, **(Mohammed and Fawzi, 2016)** tested nine burned RC beams subjected to the effect of repeated loading (loading-unloading) for five cycles and then up to failure. Furthermore, **(Allawi, 2017)** studied composite prestressed concrete girders with an external post-tensioned technique under static and repeated loading. In this research, the beams were subjected to five loading and unloading cycles up to 75% of the ultimate load. After that, the girders were reloaded gradually until failure. Also **(Hasan and Allawi, 2019)** tested eighteen simply supported reinforced concrete beams under static and fatigue loads with displacement control technique, which were exposed to high frequency (10 Hz) by fixing the fatigue load in each cycle.



(Fathuldeen and Qissab, 2019) studied the repeated loading of RC beams strengthened with NSM CFRP strips. Fifteen NSM-CFRP beams were loaded monotonically and repeatedly. Three beams were left unreinforced as references, and the others were strengthened with NSM-CFRP strips. Each group has two beams tested under monotonic loads as a control for those tested under repeated loads. For all specimens, the loading cycles were applied until failure. The test results showed that NSM-CFRP strips boosted beams' flexural strength and stiffness. The load-carrying capacity was increased from 1.47 to 4.49 times. After repeated loading, the overall area of CFRPs increased by 1.02 times the control value. Increasing the total area of CFRP strips reduced the ductility factor to 0.71, while cumulative energy absorption increased by 1.22 times for the stronger reference specimens tested under repeated loads.

(Khalaf and Al-Ahmed, 2021) used repeated loading to investigate the behavior of the existence of large openings in reinforced concrete continuous deep beams. The range of the repeated loading varied between 30% and 70% of the ultimate load of the beam subjected to static load.

(Zhu et al., 2022) studied high-strength concrete beams reinforced with BFRP bars and steel fibers under four-point cyclic loading. Five 150×300×2100mm concrete beams were built and tested. Four BFRP-reinforced concrete beams with different reinforcement ratios (ρ_s), 0.56%, 0.77%, 1.15%, and 1.65%, and one conventional steel-reinforced concrete beam were tested. Cracking, failure mechanisms, load deflection, residual deformation, and stiffness degradation were examined. An increase in ρ_s restrained fracture widths, deflections, and residual deformation while increasing beams' flexural bearing capacity. The bearing capacity was reduced by 10% in the third cycle compared to the first displacement cycle. Stiffness degraded quickly before failing. Higher ρ_s beams have higher residual stiffnesses.

The repeated load was applied by incremental loads gradually up to (75%) of the ultimate load level of the control specimen and then released the load gradually to zero with (5 cycles) of loading-unloading.

EXPERIMENTAL PROGRAM AND INSTRUMENTATION

2.1 Specimens Configuration

Four composite reinforced concrete specimens which were cast in different configurations. The overall length of the specimens was 3000mm with a support location of 125mm from each end of the beam giving a clear span of 2750mm. All specimens have the same cross-sectional dimensions, the beam width is (200 mm), and the total height of the beam is (300 mm) (see

Figure 1). The arrangement of reinforcements consists of 2 ϕ 16 mm rebars as longitudinal bottom reinforcement and 2 ϕ 10 mm rebars as top reinforcement. Stirrups of ϕ 10 mm spaced every 125 mm c/c were used as shear reinforcement.

The specimen NR-R was used as a reference specimen without additional reinforcement. The specimen CG-R was reinforced with pultruded GFRP I-beams positioned at the centroid of the cross-section (see

Figure 1-b). CGC-R was a composite specimen of GFRP with shear connectors provided in the top flange of the GFRP I-section in the specimen. The last specimen CS-R, was reinforced with a steel I-section positioned at the center of the cross-section (see

Figure 1-d). The diameter of these connectors was 12 mm, with a height of 70 mm and a spacing of 375 mm. Shear connectors were stiffened with washers and nuts after being inserted through drilled holes on both sides of the top flange of the GFRP beam (see **Figure 1-c).**

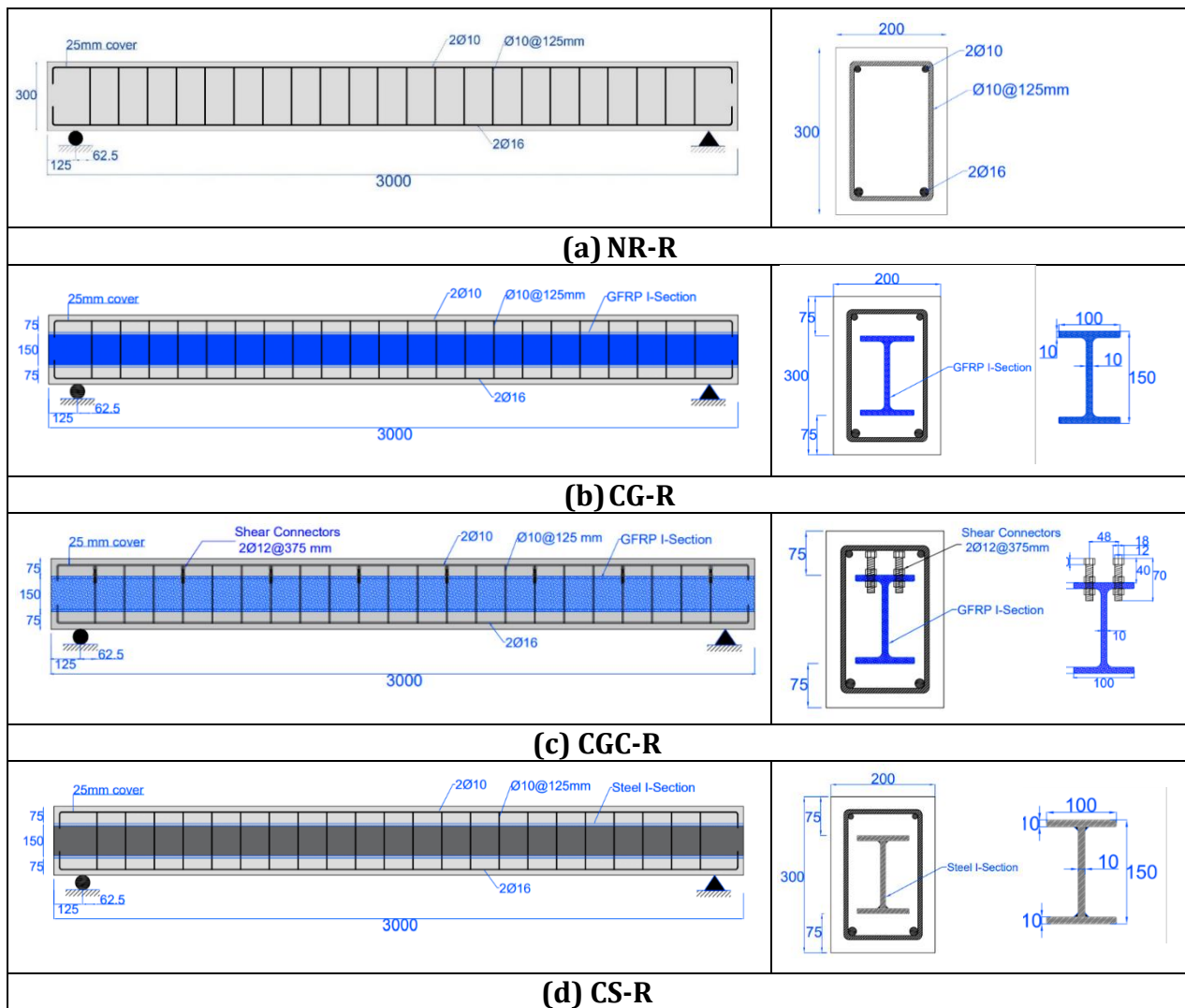


Figure 1. Details of specimens

2.2 Materials Preparation

Normal-weight concrete with a cylindrical compressive strength of about 25 MPa was produced for casting the test specimens. The yield stress and ultimate strength of steel reinforcements for a bar diameter of 16 mm were 520.73 MPa and 687.07 MPa, respectively; for a bar diameter of 10 mm, were 407.7 MPa and 465.63 MPa, and 375.9 MPa and 479.63 MPa for steel plate that was used to fabricate the steel I-section. The GFRP compressive and tensile strengths were 326.14 MPa and 347.5 MPa, respectively.

2.3 Test Setup and Instrumentations

The experimental program consisted of four composite reinforced concrete beams subjected to a non-reversed repeated loading regime depending on the ultimate load of specimens subjected to static load. The applied load was performed using an electric hydraulic jack with a 1000 kN capacity controlled using a 1000 kN load cell (see **Figure 2**). The repeated loading test sequence was started from zero value up to a certain cracking load, and then specimens were unloaded. After that, they were reloaded gradually again with a 5 kN load increment, up to a maximum of 75% of the ultimate static failure load. Then the load was gradually released to zero for five loading and unloading cycles. After that, the specimens were reloaded gradually until failure. In all specimens, the test was terminated when deflection increased dramatically under an approximately constant load.

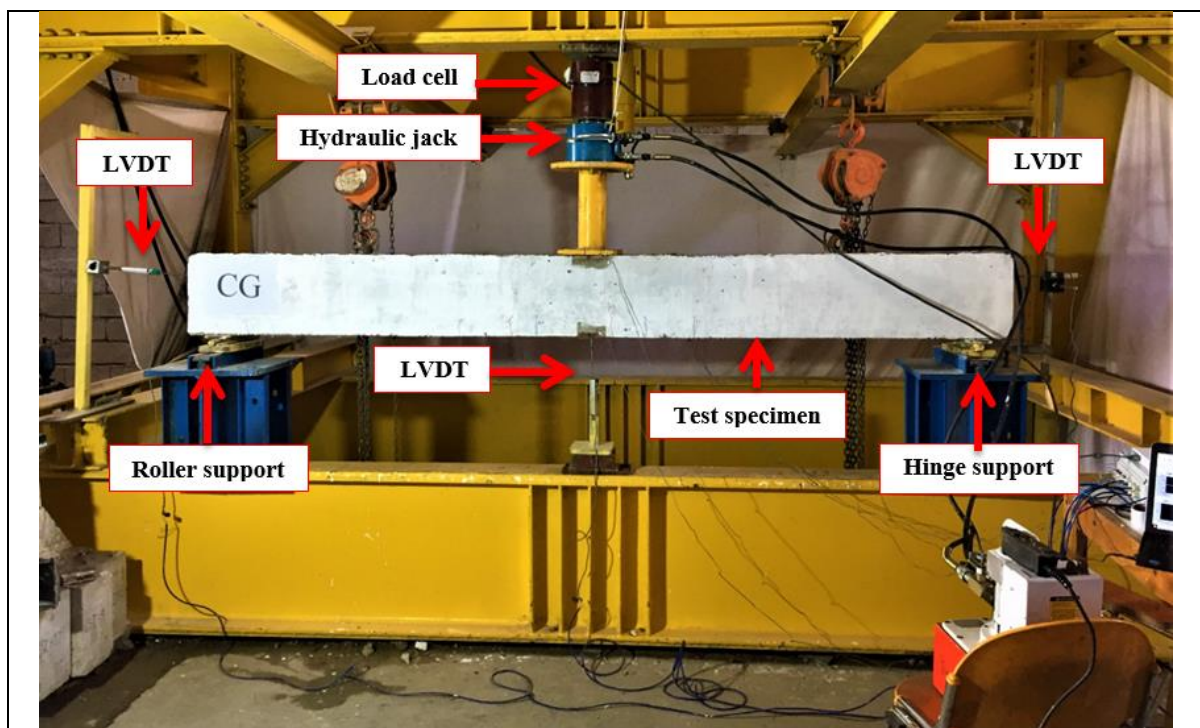


Figure 2. Setup of the test

2.4 Test Results

The simply supported four composite beams were loaded under a three-point load. The repeated test program included testing reinforced specimens loaded with a concentrated repeated load of five cycles. At the beginning of the test, each specimen was loaded with a monotonic concentrated load till a certain cracking load was reached. The specimens were then unloaded; after that, they reloaded gradually again with a 5 kN load increment up to a maximum of (75%) of the ultimate static failure load which was tested by (**Ibrahim et al, 2022**). Then loading was released gradually to zero with five loading and unloading cycles, as shown in

Figure 03. After that, the specimens were reloaded gradually until failure. In all specimens, the test was terminated when deflection increased dramatically under an approximately constant load. The test results were divided into five parts:



- Load-deformation behavior.
- Crack propagation and failure mode.
- Residual Deflection Response.
- Load-strain relations.
- Ductility

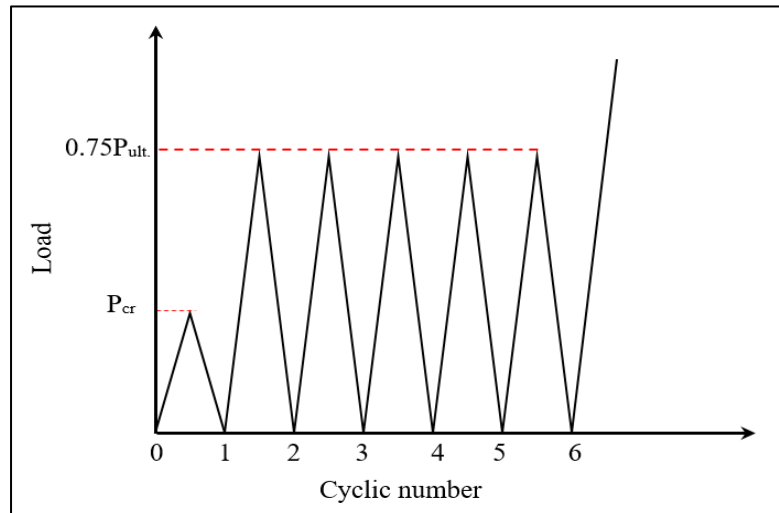
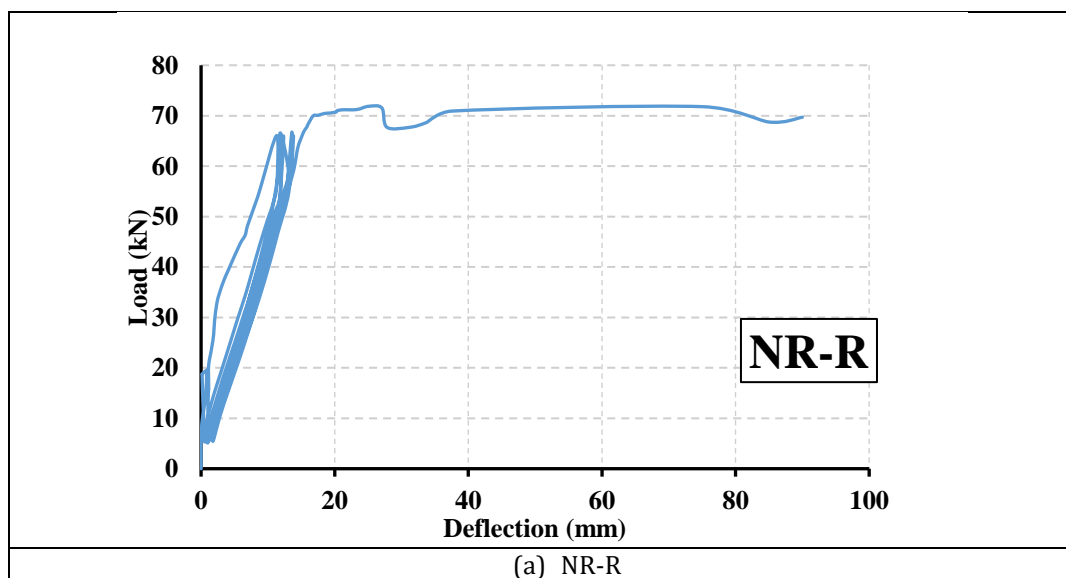


Figure 03. Scheme of Applying the Repeated Loading

2.4.1 Load –Deformation Behavior

The load-deflection curves for the beam specimens tested under the effect of repeated loads are shown in Error! Reference source not found. and Table 1 Summary of the repeated loading test results.



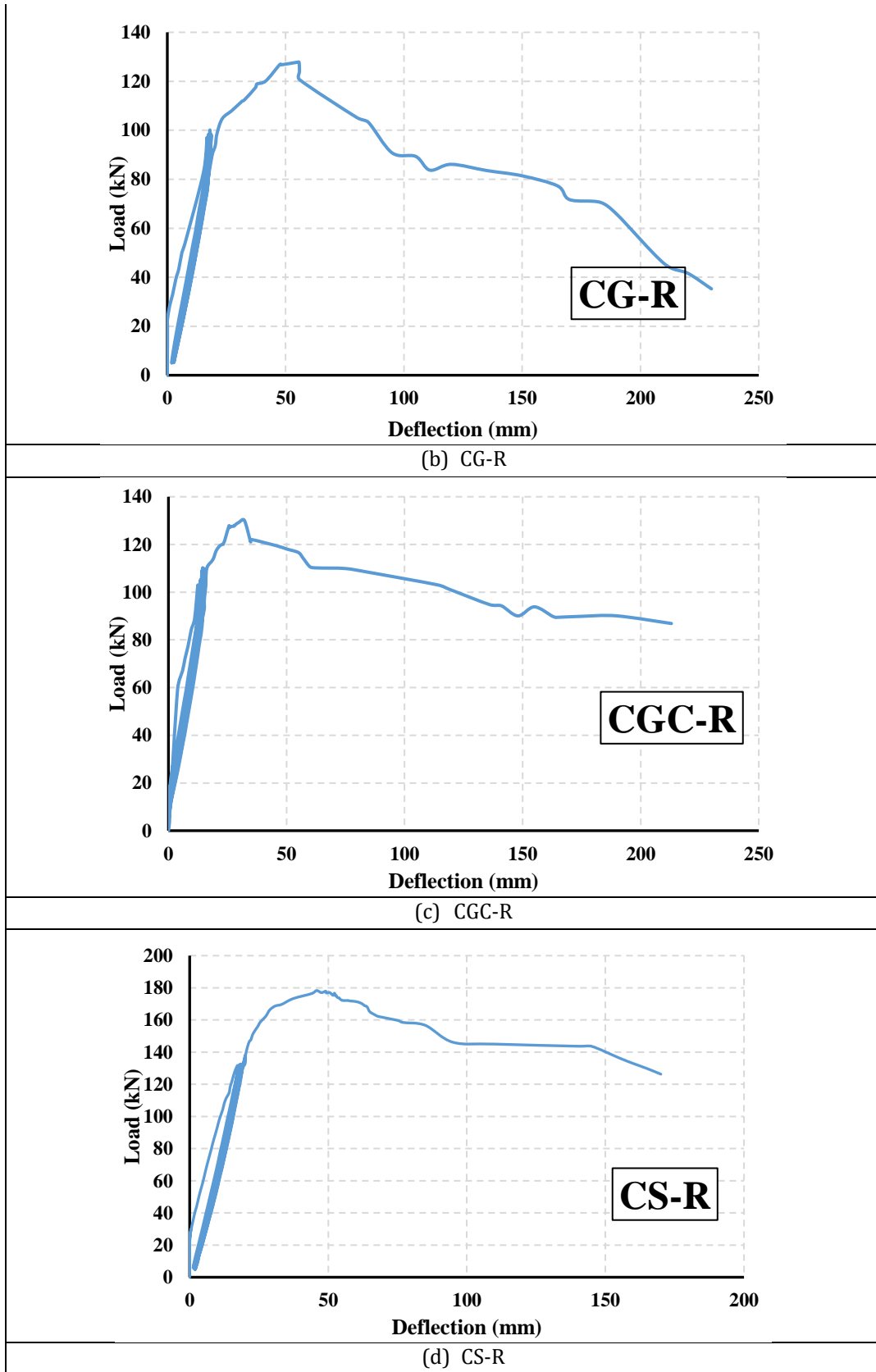


Figure 4 Load-deflection curves of the repeated test specimens.

Table 1 Summary of the repeated loading test results.

Specimen	First crack load P_{cr} (kN)	Deflection at first crack load Δ_{cr} (mm)	Yield load P_y (kN)	Deflection at yield load Δ_y (mm)	Ultimate load P_u (kN)	Deflection at ultimate load Δ_u (mm)
NR-R	19.56	0.84	66.05	10.1	71.86	25.06
CG-R	20.93	0.154	103.5	19.9	127.78	25.06
CGC-R	20.64	0.45	112	13.7	130.12	32.14
CS-R	29.85	0.42	135	19.2	178.32	45.79

2.4.2 Cracks Propagation and Failure Modes

The first flexural crack appears at the middle third of the beams whenever the tensile stresses exceed the modulus of rupture of concrete, this crack occurred at the load range of (15.86 % to 27.22 %) from the ultimate load capacity of the repeated-tested specimens, and this crack develops slowly across the width of the beam as shown in **Figure 5-8**. The crack pattern of the samples applying to the repeatedly loaded was almost the same as in the samples tested under static load. However, more cracks appeared when the number of loading cycles increased, and their width grew. It was shown in Table 2 that the ultimate load of the composite specimens CG-R, CGC-R, and CS-R increases by about (77.82 %, 81.07 %, and 148.15 %) relative to the NR-R specimen. Table 2 shows cracking and ultimate load for repeated load specimens.

Table 2. Cracking and Ultimate Loads of Repeated-Tested Specimens

Specimen	Crack load P_{cr} (kN)	Ultimate load P_u (kN)	P_{cr}/P_u %	Increase in First Cracking Load Concerning Reference %	Increase in Ultimate Load Concerning Reference %
NR-R	19.56	71.86	27.22	---	---
CG-R	20.93	127.78	16.38	7.00	77.82
CGC-R	20.64	130.12	15.86	5.52	81.07
CS-R	29.85	178.32	16.74	52.61	148.15





Figure 5 Failure mode of the NR-R specimen

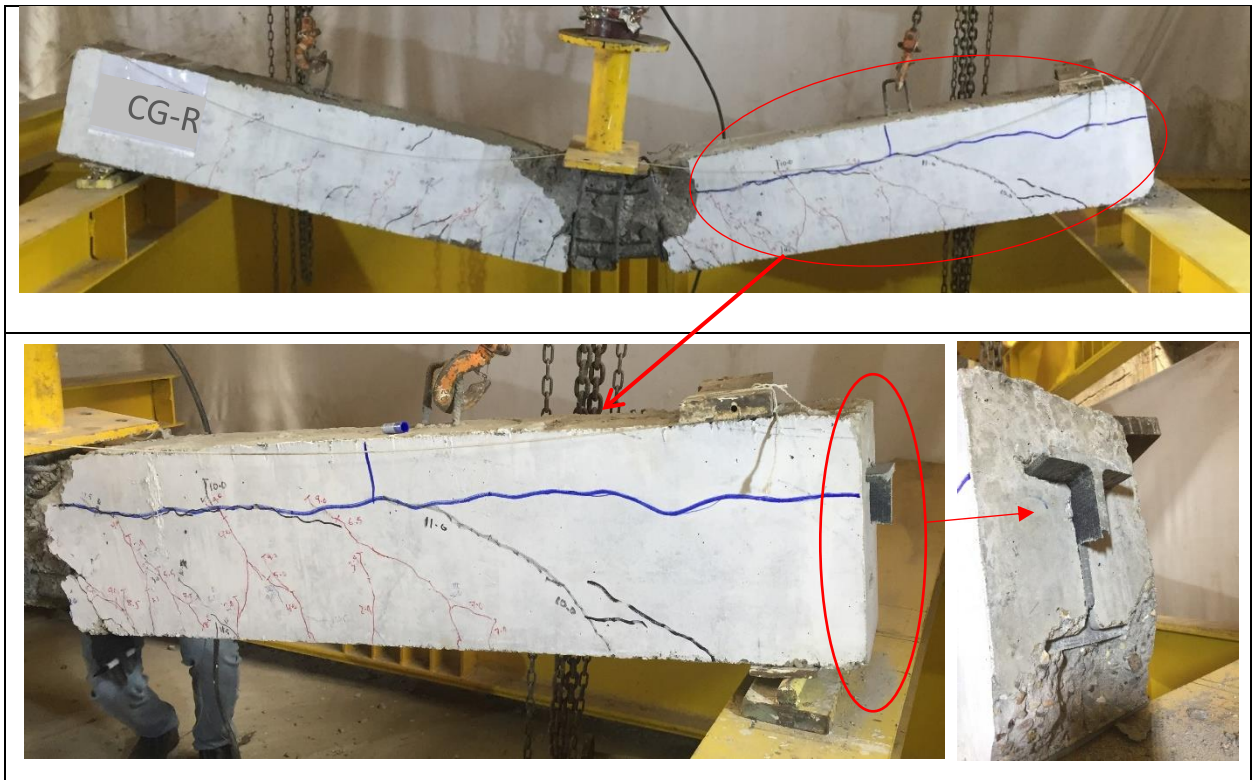
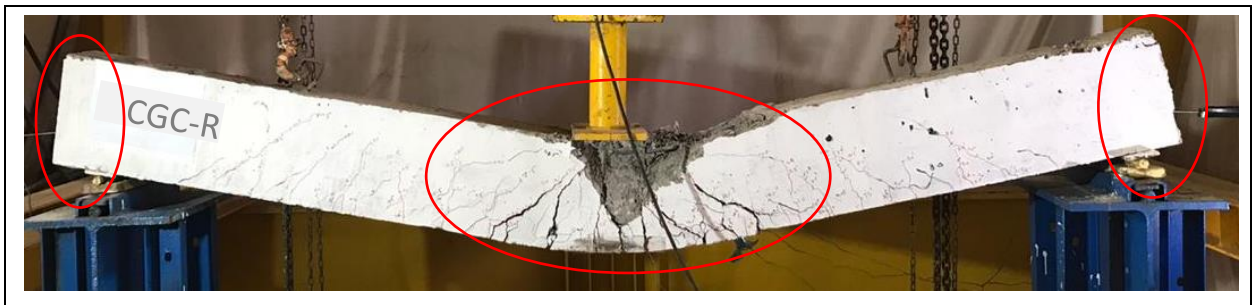


Figure 6 Failure mode of the CG-R specimen



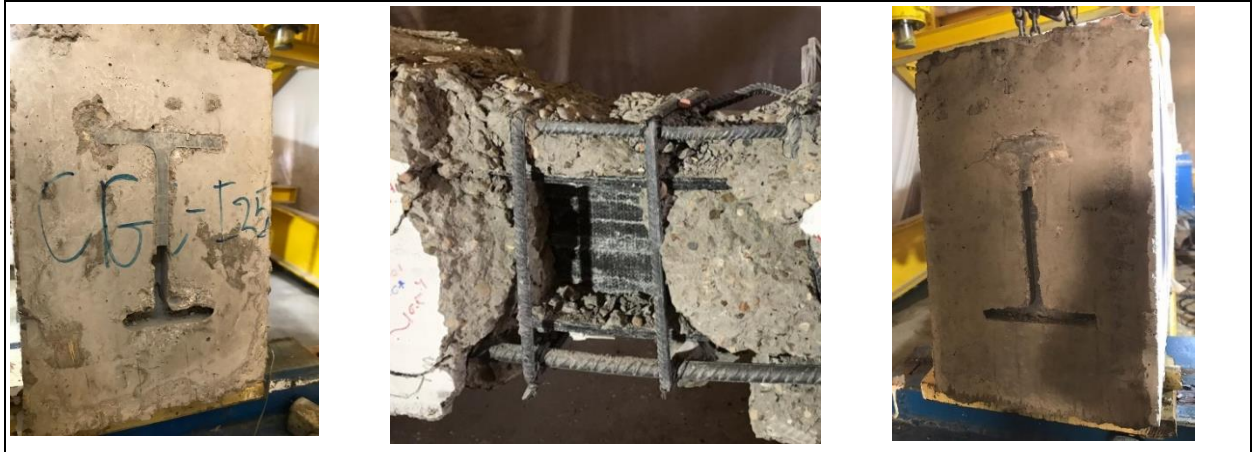


Figure 7 Failure mode of the CGC-R specimen



Figure 8 Failure mode of the CS-R specimen



As expected and explained before, the ultimate load capacity increases for the composite specimens CG-R, CGC-R, and CS-R, respectively, concerning the specimen NR-R.

For the NR-R specimen, after loading and unloading five cycles up to the ultimate loads, specimens showed the flexural failure mode by yielding steel reinforcement and compression concrete crushing and propagation of flexural cracks. After that, a sudden fracture in tensile steel reinforcement happened, leading to the collapse of the specimen, as shown in **Figure 5**.

For composite specimens, CG-R and CGC-R flexural cracks gradually spread in the midspan region in the first cycle after reaching the cracking load. No more cracks appeared for the last four cycles, but the previous cracks began to elongate. After the five cycles, concrete crushing started at a yield load; the number of cracks increased with loading increment; wider cracks were developed. The deflection began to overgrow when the applied load reached 127.78 kN and 130.12 kN for specimens CG-R and CGC-R, respectively. After applying the ultimate loads, the compression steel rebars were bent over. The concrete cover was spalled, accompanied by a loud noise produced by the initial inter-laminar failure and rupture of the GFRP profile, as illustrated in Fig. 6 and Fig. 7. Finally, the testing was stopped due to slipping and crushing in the GFRP profile. The applied loads began to drop gradually. The web of the GFRP beam crashed, resulting in longitudinal shear failure.

At the end of the first cycle for the composite specimen with the steel I-section CS-R, flexural cracks grew in the middle of the span. For the four cycles, shear cracks appeared: no more flexural cracks appeared, but the previous cracks began to elongate. After the five cycles, concrete crushing started at a yield load of 135 kN. At the maximum load of 178.32 kN, the number of cracks increased with loading increment; wider cracks were developed. The test was terminated due to steel yielding followed by buckling and twisting in the steel I-section inside the concrete. This caused radial cracks at the end flange on the beam sides and crushing at the end supports' position, as shown in **Figure 8**.

2.4.3 Residual Deflection Response

In the loading and unloading process, the load-deflection curve's ascending and descending portions take different patterns; the difference between the two is commonly referred to as residual deflection. The results of the tests showed that, for all the specimens, the amount of deflection at the same point and load increment increased as the number of loading cycles increased. This means the specimen did not return to its original position when the load was released, and a residual deflection was observed. As shown in **Table 3**, the test results for the composite specimens CG-R, CGC-R, and CS-R showed that the residual deflection was 12.52 %, 15.29 %, and 21.2 % less than that of the reference beam NR-R. This could be because of the benefits of high stiffness of specimens, which led to increased ductility of concrete and decreased permanent deformations. It was noticed that the most residual deflection happened in the first cycle, while **Figure 9** shows that the differences in residual deflection between the last four cycles were not as significant as the difference between the first and second cycles.



Table 3. Residual deflection of the repeated load test specimens at the first load cycle.

Specimen	Residual deflection (mm)	Decrease in residual deflection %
NR-R	1.512	----
CG-R	1.32	12.52
CGC-R	1.28	15.29
CS-R	1.191	21.2

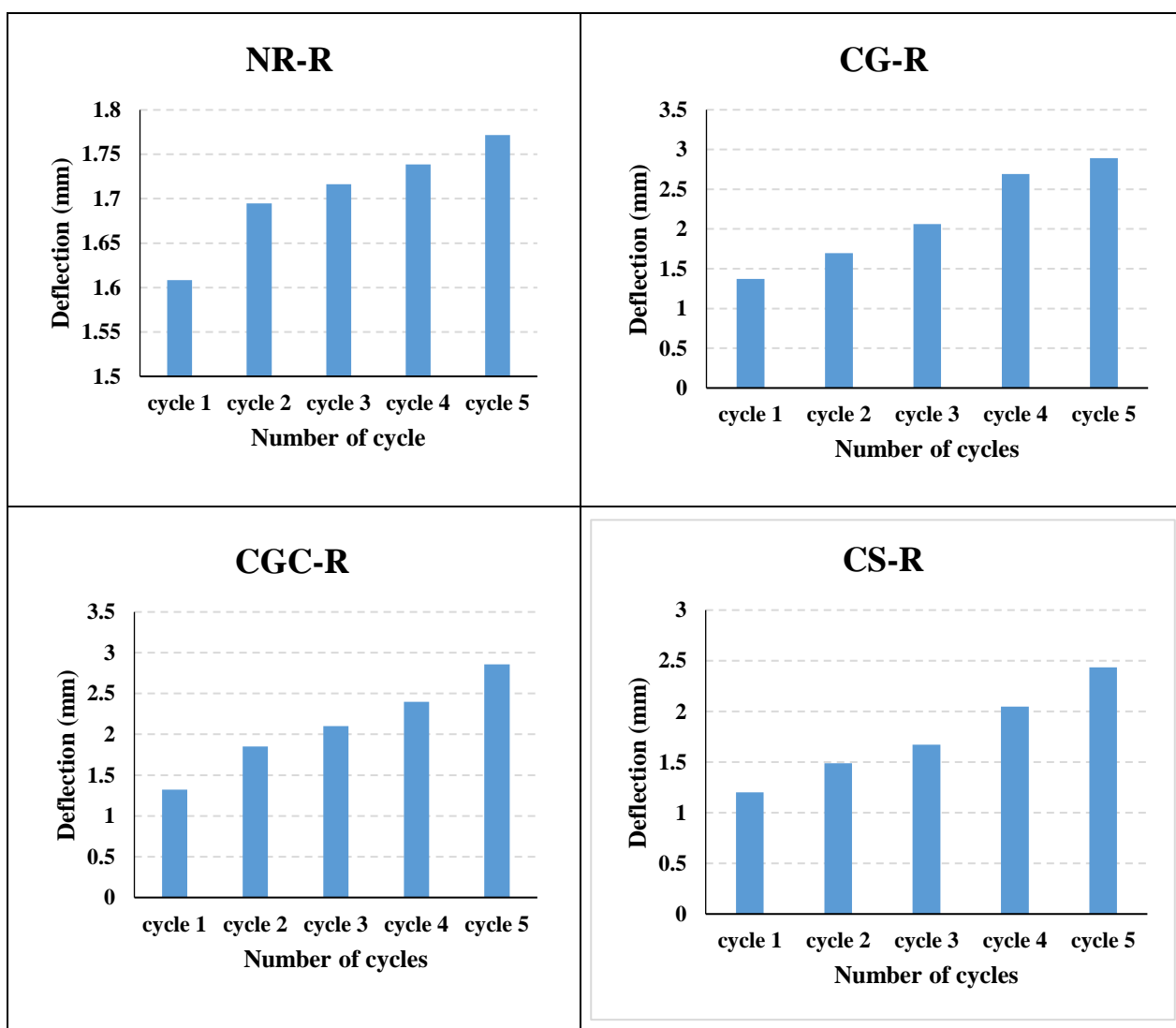


Figure 9. The residual deflection at different cycles at the minimum loads of the repeated cycles

2.4.4 Load-strain relation

The same locations of the strain gauges for the specimens tested under static load are adopted to measure and represent the load-strain relations of the specimens tested under repeated load. **Figure 10-Figure 13** illustrates the maximum compressive strain of the concrete was 0.005 mm/mm, while the GFRP within the elastic range has a tensile strain of 0.006 at the ultimate load level of the specimens CG-R and CGC-R. And for the CS-R specimen, the I-steel profile's maximum compressive and tensile strain was about 0.025 mm/mm.

The failure load of the composite specimens with GFRP CG-R and CGC-R was determined from the maximum strain value recorded in the web of the GFRP profile.

Regarding the load-strain relation **Figure 10-Figure 13**, it was noticed that the most significant effect of the repeated load was in the first cycle. In contrast, it is clear from **Figure 10** that the differences in the strains between the last four cycles were relatively small in comparison with the difference between the first and the second cycles.

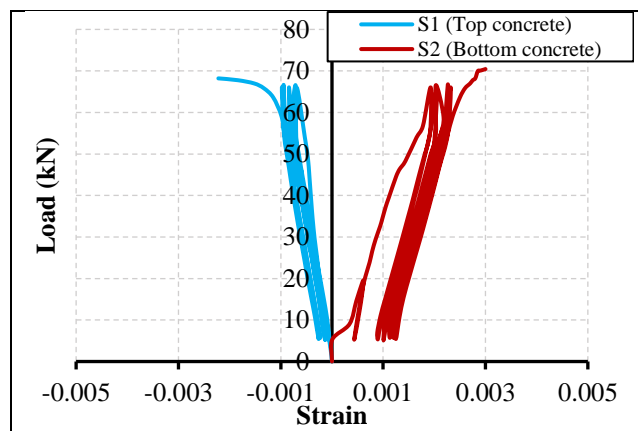


Figure 10. Recorded strains as a function of the applied loads for the NR-R specimen.

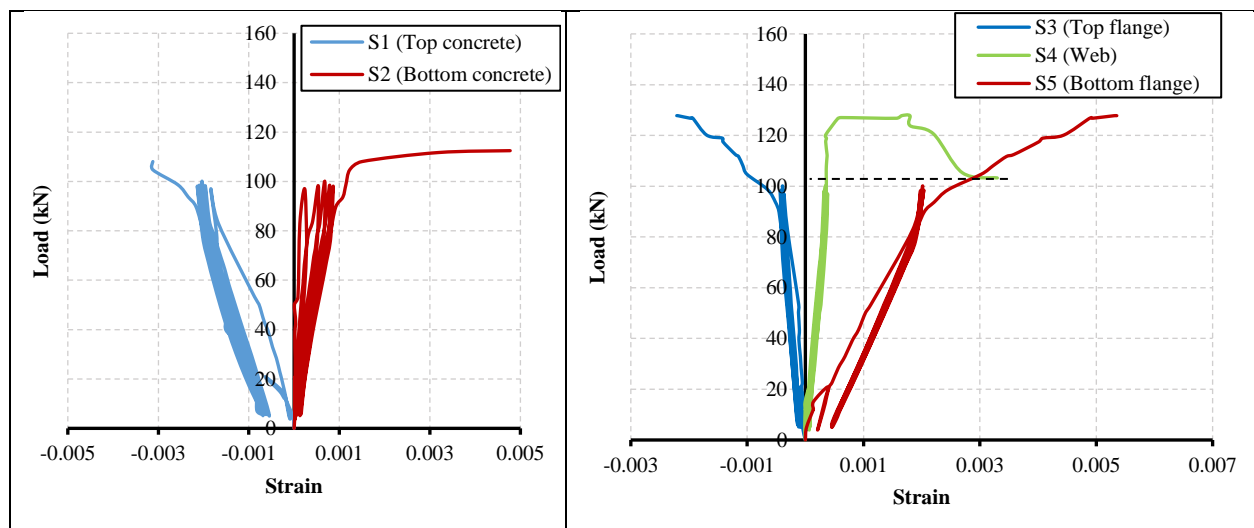


Figure 11. Recorded strains as a function of the applied loads for the CG-R specimen.

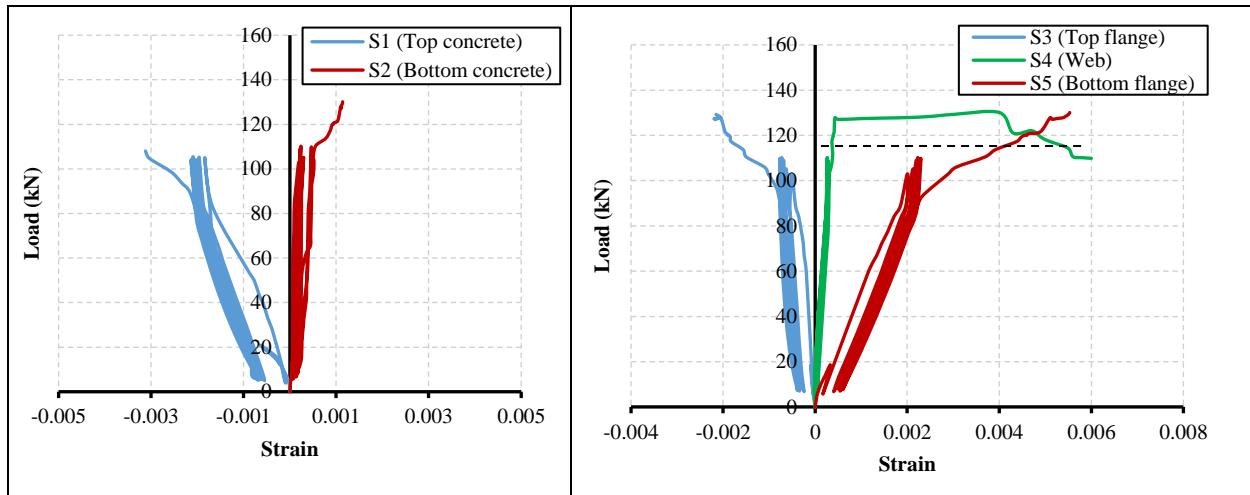


Figure 12. Recorded strains as a function of the applied loads for the CGC-R specimen.

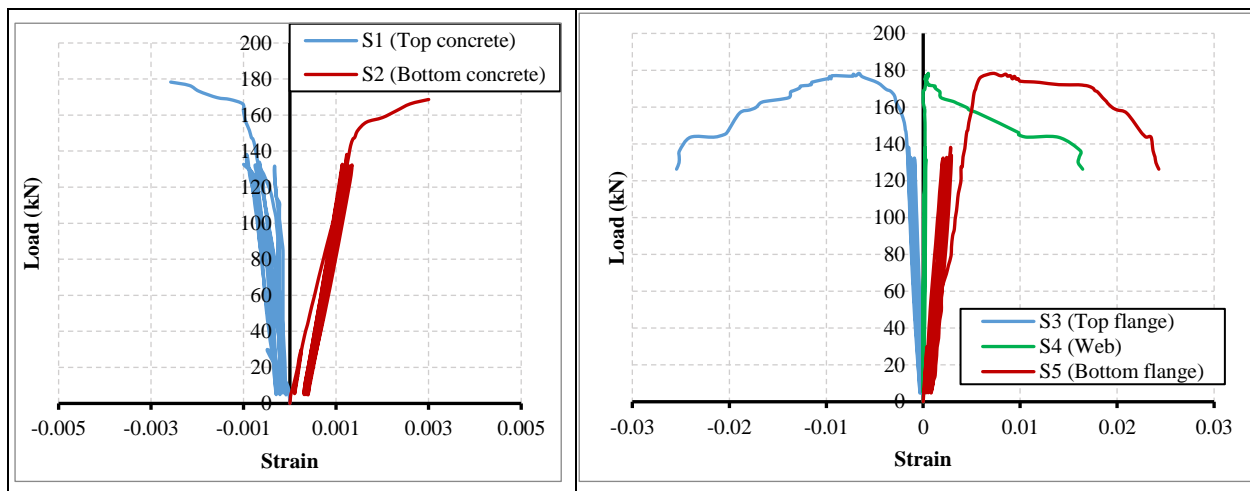


Figure 13. Recorded strains as a function of the applied loads for the CS-R specimen.

2.4.5. Ductility

Ductility is a requirement for structural design in most design codes. It is defined in RC structures as the ultimate deformation relative to the yield point deformation, which is usually caused by steel reinforcement. Typical ductility definitions do not apply to GFRP-reinforced structures because of the linear strain-stress relationship of GFRP. Several approaches have been presented for determining the ductility index of GFRP-reinforced structures. The most common module was proposed by (Naaman AE, 1995), as illustrated in Figure 14. It has been used in some previous studies (Wang and Belarbi, 2005), (Oudah and El-Hacha, 2012), (Aziz and Taha, 2013), (Hadi and Yuan, 2017), and (Mahmood et al. 2022). In this module, the ductility index μ_E can be calculated in the following equation:

$$\mu_E = \frac{1}{2} \left(\frac{E_{tot}}{E_{el}} + 1 \right) \tag{1}$$

Where:

E_{tot} : the total energy, which was calculated by the area under the load-midspan deflection curve up to the failure load.

E_{el} : the elastic energy, which was calculated as the triangle area produced at the failure load P_{fail} by the line with the weighted average slope of the two starting straight lines S_1 and S_2 of the load-deflection relationship.

P_1 and P_2 : are the loads at the end of the initial two lines, respectively, as illustrated in **Figure 14**.

Energy ductility is also defined as the ability to absorb inelastic energy without compromising load capacity. Higher inelastic energy absorption equates to higher ductility of the same system. The GFRP and the steel I-section improve the system's ductility significantly compared to the reference specimens. The ductility index depends on specimens' elastic and total energy amounts are shown in **Table 4**. It was observed from **Table 4** that for all the composite beams, the ductility factor increased as compared to the reference beam. The greatest increases were recorded at the composite beam CGC-R, which was approximately 156%, while specimens CG-R and CS-R were increased by 148.6% and 96%, respectively.

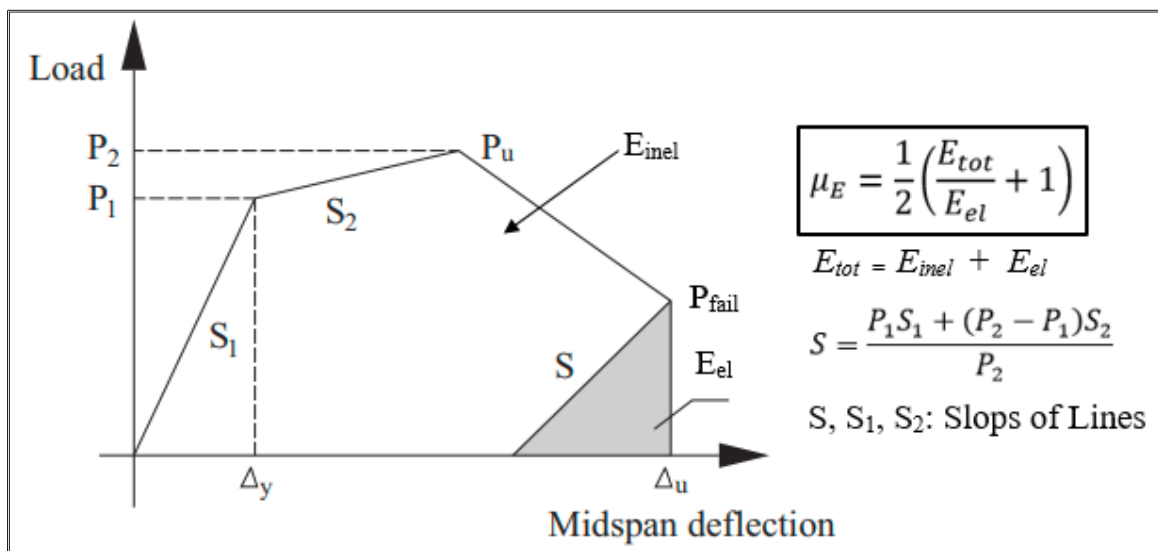


Figure 14 Definition of Ductility Index by Namman AE, 1995



Table 4 Energy Ductility Index of Specimens

Specimen	S1	S2	S	Total Energy E_{tot} (kN.mm)	Elastic Energy E_{el} (kN.mm)	Energy Ductility index μ_E	Increasing in Ductility Index %
NR-R	6.54	0.39	6.04	1686.89	402.02	2.59	---
CG-R	5.53	4.61	5.11	11317.54	1042.71	5.93	148.6
CGC-R	8.18	0.98	7.17	9386.6	841.69	6.08	156.2
CS-R	7.03	1.63	5.72	14393.71	2008.57	4.08	96.0

CONCLUSION

1. The test results for the composite specimens with GFRP and steel I-section showed that the residual deflection ranged from 12.5% to 21.20% less than the reference beam.
2. Compared to the reference specimen, the ultimate load of the composite specimen increased by approximately 77.82% for the composite with GFRP, 81.07% for the composite of the GFRP beam with studs, and 148.15% for the composite beam with steel.
3. The ductility index increased for the composite beams relative to the reference specimen by 156.2% for a composite beam with GFRP with shear connectors, 148.6% for composite beams with GFRP without connectors, and 96% for the composite beam with a steel I-section.

ACKNOWLEDGMENT

The authors gratefully appreciate and gratitude the staff of the Structural Laboratory of the Civil Engineering Department at the University of Baghdad, Iraq, for their support in the experimental part of the research. Also, the authors are grateful to thank the Consulting Engineering Bureau at the University of Baghdad (CEB-UB) for assistance in fulfilling the material test.

REFERENCE

Abbas A. Allawi. 2017. "Behavior of Strengthened Composite Prestressed Concrete Girders under Static and Repeated Loading." *Advances in Civil Engineering* 2017(December).

Abbas A. Allawi, Hussain Askar Jabir. 2016. "Response of Laced Reinforced Concrete One Way Slab to Repeated Loading." *Journal of Engineering* 22(09): 36–54.

Allawi, Abbas A., and Safaa I. Ali. 2020. "Flexural Behavior of Composite GFRP Pultruded I-Section Beams under Static and Impact Loading." *Civil Engineering Journal (Iran)* 6(11): 2143–58.

Aziz, Omar Qarani, and Bahman Omar Taha. 2013. "Flexure Behavior of High Strength Concrete (HSC) Beams Reinforced With Carbon Fiber Reinforced Polymer (CFRP) Rebars With and Without Chopped Carbon Fiber (CCF)." *International Journal of Scientific Research in Knowledge* 1(6): 123–39.

Enas M. Mahmood, Abbas A. Allawi and Ayman El-Zohairy. 2022. "Flexural Performance of Encased Pultruded GFRP I-Beam with High Strength Concrete under Static Loading."



materials 15(13): 1–20.

Fathuldeen, Saja Waleed, and Musab Aied Qissab. 2019. "Behavior of RC Beams Strengthened with NSM CFRP Strips under Flexural Repeated Loading." *Structural Engineering & Mechanics* 70(1): 67–80.

Hadi, Muhammad N.S., and Jian Song Yuan. 2017. "Experimental Investigation of Composite Beams Reinforced with GFRP I-Beam and Steel Bars." *Construction and Building Materials* 144: 462–74. <http://dx.doi.org/10.1016/j.conbuildmat.2017.03.217>.

Hasan, Haifaa dhamad, and Abbas A. Allawi. 2019. "Flexural Performance of Laced Reinforced Concrete Beams under Static and Fatigue Loads." *Journal of Engineering* 25(10): 134–53.

Mohammed R. Khalaf, Ali Al-Ahmed. 2021. "Effect of Large Openings on the Behavior of Reinforced Concrete Continuous Deep Beams under Static and Repeated Load." In *E3S Web of Conferences*, , 1–8.

Naaman AE, Jeong SM. 1995. "Structural Ductility of Concrete Beams Prestressed with FRP Tendons." *Proc., 2nd Int. RILEM Symp. (FRPRXS-2), Non-Metric (FRP) Reinforcement for Concrete Structures* RILEM, Bag.

Oudah, Fadi, and Raafat El-Hacha. 2012. "A New Ductility Model of Reinforced Concrete Beams Strengthened Using Fiber Reinforced Polymer Reinforcement." *Composites Part B: Engineering* 43(8): 3338–47. <http://dx.doi.org/10.1016/j.compositesb.2012.01.071>.

Safaa I. Ali, Abbas A. Allawi. 2021. "Effect of Web Stiffeners on The Flexural Behavior of Composite GFRP- Concrete Beam Under Impact Load." *Journal of Engineering* 27(3): 73–92.

Shatha Dheyaa Mohammed, Nada Mahdi Fawzi. 2016. "Fire Flame Influence on the Behavior of Reinforced Concrete Beams Affected by Repeated Load." *Journal of Engineering* 22(9): 206–23.

Sivagamasundari, R., and G. Kumaran. 2008. 2 The Open Civil Engineering Journal "A Comparative Study on the Flexural Behaviour of One-Way Concrete Slabs Reinforced with GFRP Reinforcements and Conventional Reinforcements When Subjected to Monotonic and Repeated Loading."

Teghreed H. Ibrahim, Abbas A. Allawi, and Ayman El-Zohairy. 2022. "Experimental and FE Analysis of Composite RC Beams with Encased Pultruded GFRP I-Beam under Static Loads." *Advances in Structural Engineering*: 1–17.

Teghreed H. Ibrahim, Abbas A. Allawi and Ayman El-Zohairy. 2022. "Impact Behavior of Composite Reinforced Concrete Beams with Pultruded I-GFRP Beam." *materials* 15(2): 1–24.

Wang, H. and Belarbi, A. 2005. "Flexural Behavior of Fiber-Reinforced-Concrete Beams Reinforced with FRP Rebars." *ACI Structural Journal* SP-230: 895–914.

Zhu, Haitang, Chuanchuan Li, Shengzhao Cheng, and Jiansong Yuan. 2022. "Flexural Performance of Concrete Beams Reinforced with Continuous FRP Bars and Discrete Steel Fibers under Cyclic Loads." *Polymers* 14(7).